






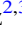
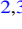






GW190412 as a Third-generation Black Hole Merger from a Super Star Cluster

Carl L. Rodriguez¹ , Kyle Kremer^{2,3} , Michael Y. Grudić^{2,3} , Zachary Hafen^{2,3} , Sourav Chatterjee⁴ ,
Giacomo Fragione^{2,3} , Astrid Lamberts⁵ , Miguel A. S. Martinez^{2,3} , Frederic A. Rasio^{2,3} , Newlin Weatherford^{2,3} , and
Claire S. Ye^{2,3} 

¹ Harvard Institute for Theory and Computation, 60 Garden Street, Cambridge, MA 02138, USA; carl.rodriguez@cfa.harvard.edu

² Department of Physics & Astronomy, Northwestern University, Evanston, IL 60208, USA

³ Center for Interdisciplinary Exploration & Research in Astrophysics (CIERA), Northwestern University, Evanston, IL 60208, USA

⁴ Tata Institute of Fundamental Research, Homi Bhabha Road, Navy Nagar, Colaba, Mumbai 400005, India

⁵ Université Côte d’Azur, Observatoire de la Côte d’Azur, CNRS, Laboratoire Lagrange, Laboratoire ARTEMIS, France

Received 2020 May 6; revised 2020 May 19; accepted 2020 May 22; published 2020 June 9

Abstract

We explore the possibility that GW190412, a binary black hole merger with a non-equal-mass ratio and significantly spinning primary, was formed through repeated black hole mergers in a dense super star cluster. Using a combination of semianalytic prescriptions for the remnant spin and recoil kick of black hole mergers, we show that the mass ratio and spin of GW190412 are consistent with a binary black hole whose primary component has undergone two successive mergers from a population of $\sim 10M_{\odot}$ black holes in a high-metallicity environment. We then explore the production of GW190412-like analogs in the CMC Cluster Catalog, a grid of 148 N -body star cluster models, as well as a new model, *behemoth*, with nearly 10^7 particles and initial conditions taken from a cosmological MHD simulation of galaxy formation. We show that, if the spins of black holes born from stars are small, the production of binaries with GW190412-like masses and spins is dominated by massive super star clusters with high metallicities and large central escape speeds. While many are observed in the local universe, our results suggest that a careful treatment of these massive clusters, many of which may have been disrupted before the present day, is necessary to characterize the production of unique gravitational-wave events produced through dynamics.

Unified Astronomy Thesaurus concepts: Gravitational wave sources (677); Astrophysical black holes (98); Stellar mass black holes (1611); Globular star clusters (656); Star clusters (1567); Stellar mergers (2157)

1. Introduction

Since 2015, the LIGO and Virgo gravitational-wave (GW) observatories have reported the detection of 11 binary black hole (BBH) mergers (Aasi et al. 2015; Acernese et al. 2015; Abbott et al. 2019b; The LIGO Scientific Collaboration, & the Virgo Collaboration 2020), with independent analyses (Nitz et al. 2020; Venumadhav et al. 2020) identifying several additional candidates. However, the majority of these previous events have been composed of black holes (BHs) with near-equal component masses.⁶ This complemented theoretical models of BBH formation through either isolated binary evolution (e.g., Dominik et al. 2012; De Mink & Mandel 2016; Belczynski et al. 2020) or dynamical formation (e.g., Rodriguez et al. 2016c) that strongly preferred BBH mergers with mass ratios near unity (Abbott et al. 2016, 2019a). However, the first BBH merger announced from LIGO/Virgo’s third observing run—GW190412, a $\sim 30M_{\odot} + 8M_{\odot}$ binary—bucks this trend with a mass ratio of nearly four-to-one (The LIGO Scientific Collaboration, & the Virgo Collaboration 2020). This particular configuration allows for the recovery of higher-order modes in the gravitational waveform, which strongly constrains the dimensionless spin magnitude of the primary BH to $0.43^{+0.16}_{-0.26}$, the largest spin of a premerger BH measured through GWs.

Although such systems can potentially be formed through isolated binary evolution (e.g., Mandel & Fragos 2020; Olejak et al. 2020) or through dynamical exchanges in young, low-

mass clusters (e.g., Di Carlo et al. 2020), an obvious way to produce such systems is through hierarchical mergers of BHs in a dense star cluster. If two low-spinning, “first-generation” (1G) BHs were to merge in a cluster with a sufficiently large escape speed, their “second-generation” (2G) merger product will remain in the cluster, where it can find another partner and merge again. This scenario has been explored extensively in the literature (Fishbach et al. 2017; Gerosa & Berti 2017) in the context of globular clusters (GCs, Rodriguez et al. 2018, 2019), nuclear star clusters (NSCs; Miller & Lauburg 2009; O’Leary et al. 2009; Antonini & Rasio 2016; Antonini et al. 2019), and the disks of active galactic nuclei (Bartos et al. 2017; Stone et al. 2017; Secunda et al. 2019; Yang et al. 2019a, 2019b; McKernan et al. 2020). However, the merger of just a single pair of BHs with similar masses and low spins produces BHs with dimensionless spins of ~ 0.69 (Berti & Volonteri 2008; Tichy & Marronetti 2008; Kesden et al. 2010; Fishbach et al. 2017), a value outside the 90% posterior probability for the primary spin of GW190412.

In this Letter we show that GW190412 is instead consistent with a “third-generation” (or 3G) BBH merger whose primary BH was created from two successive BBH mergers. In Section 2, we argue based on previous work in both cluster dynamics and numerical relativity that the most likely dynamical source for GW190412 is a massive, high-metallicity cluster with a large escape speed, and that the retention of 3G BHs in the cluster automatically selects for BHs with spins near the median of the GW190412 primary spin posterior. In Sections 3 and 4, we use collisional models of star clusters, including a new, massive cluster—*behemoth*—which

⁶ Though see Venumadhav et al. (2020) for a description of GW170202, a BBH merger candidate with a mass ratio of two-to-one.

produces multiple GW190412-like progenitors that merge in the local universe. Finally, we conclude by discussing how such massive clusters exist in the local universe, but are strongly dependent on the galactic environments they inhabit.

2. Clues to the Formation of GW190412

Dense star clusters come in a wide range of initial masses, metallicities, and concentrations. We have previously shown that dense star clusters can naturally form heavy $30M_{\odot} + 30M_{\odot}$ BBHs (e.g., GW150914 Rodríguez et al. 2016b) as well as lower-mass $10M_{\odot} + 10M_{\odot}$ binaries (e.g., GW151226, Chatterjee et al. 2017). The key determining factor between these two mass regimes is the cluster metallicity: low-metallicity systems such as classical globular clusters (GCs, e.g., Harris 1996) are optimal for producing $\sim 30M_{\odot}$ BHs, while higher-metallicity clusters such as open clusters (OCs) and super star clusters (SSCs; Portegies Zwart et al. 2010, and references therein) preferentially produce lower-mass BHs. This difference in the BH mass distribution arises from the strength of stellar winds in massive stars; higher metallicity stars experience stronger winds (e.g., Vink et al. 2001) and correspondingly larger mass loss rates, resulting in less massive BH progenitors prior to stellar collapse (e.g., Belczynski et al. 2010; Spera et al. 2015).

Of course, a low-metallicity GC containing many $\sim 30M_{\odot}$ BHs would still contain an even greater population of $\sim 10M_{\odot}$ BHs by virtue of the initial-mass function (IMF), so why do we discount such clusters as a potential source of GW190412-like binaries? After mass segregation is complete in a star cluster, the most massive BHs are found in the center of the cluster, where they predominantly form binaries with BHs of similar masses (Morscher et al. 2015). It is these massive BHs that primarily participate in the repeated three-body encounters that form binaries and lead to the ejection of BHs and BBHs from the cluster (e.g., Kulkarni et al. 1993; Sigurdsson & Phinney 1993). Only after the most massive objects have been ejected can the lighter BHs and neutron stars migrate into the cluster center and participate in such encounters (e.g., Morscher et al. 2015; Ye et al. 2020). Even if—in spite of mass segregation—a one-to-four mass ratio binary were to form, approximately 30%–50% of low-velocity encounters between the binary and other massive BHs would result in an “exchange” encounter, where the lower-mass BH is replaced by the interloper; see Sigurdsson & Hernquist (1993, Table 3A). To eject or merge a BBH from a GC requires 10–100 s of these low-velocity encounters,⁷ giving many opportunities for an exchange to occur (Rodríguez et al. 2016a). As long as the BBH components are sourced from a continuous BH mass distribution, mass segregation and three-body dynamics will tend to create equal-mass BBH mergers.

But when a BBH merges inside a cluster, its merger product can be retained by the cluster, where it is nearly twice as massive as the most massive 1G BHs. These 2G BHs are much more likely than their 1G progenitors to form binaries and merge again within a Hubble time, with a nearly two-to-one mass ratio between the 2G and 1G components (Rodríguez et al. 2019). Furthermore, when two BHs with similar masses merge, the spin distributions of their merger products will be

⁷ Here “low-velocity” refers to those where the interloper is moving below the critical velocity of the system, defined as the velocity where the binding energy of the binary is equal to the kinetic energy of the interloper and the binary center of mass at infinity. See Hut & Bahcall (1983).

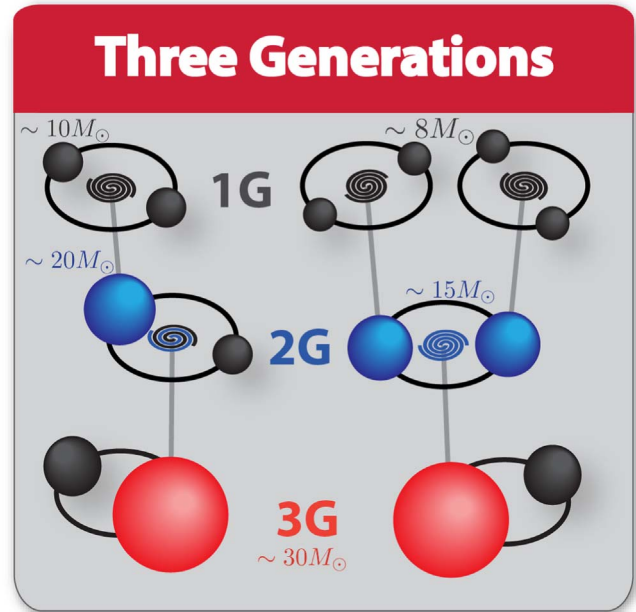


Figure 1. Cartoon merger tree of the two possible multimergers of GW190412, where the massive primary (in red) is created from the merger of either one or two 2G BHs (in blue).

peaked at 0.69 (Berti et al. 2007; Fishbach et al. 2017). This yields an obvious pathway to producing BBHs with a more massive and spinning primary. However, both a two-to-one mass ratio and $\chi_1 = 0.69$ are excluded at the 90% level for GW190412. As we will show, constructing GW190412 from low-spin 1G BHs, with its mass ratio of 0.28 and $\chi_1 = 0.43$, requires an additional merger.

In Figure 1, we show two possible pathways to forming $30M_{\odot}$ 3G BHs, where the 3G component is formed through either a 1G+2G merger (with masses $M_1 = 20M_{\odot}$, $M_2 = 10M_{\odot}$, and spins $\chi_1 = 0.69$ and $\chi_2 = 0$) or a 2G+2G merger (both with masses of $15M_{\odot}$ and spins of 0.69). In the top panel of Figure 2, we show the final spin distributions for the resultant 3G BHs, calculated by Monte Carlo sampling over all possible spin orientations of the progenitors using phenomenological fits to numerical and analytic relativity calculations for the final spin and recoil kicks of the BBH merger products (Campanelli et al. 2007; González et al. 2007; Lousto & Zlochower 2008, 2013; Barausse & Rezzolla 2009; Lousto et al. 2012). Note that these are the same distributions employed in our Cluster Monte Carlo code (Rodríguez et al. 2018, Appendix A).

The median final spins for all 1G+2G and 2G+2G mergers ($\chi_f = 0.62$ and 0.68 , respectively) are both beyond the 90% credible region for the GW190412 primary. However, if we consider only 3G BHs that receive kicks below 100 km s^{-1} , the median remnant spin decreases to 0.43 and 0.65 for 1G+2G and 2G+2G mergers, respectively, the former of which agrees perfectly with the median for the spin posterior of the GW190412 primary. This correlation between BH recoil and remnant spin is shown explicitly in the bottom panel of Figure 2: 100% of 1G+2G BBH mergers (and $\sim 30\%$ of 2G+2G mergers) with recoil kicks below $\sim 100 \text{ km s}^{-1}$ produce BHs with spins matching the LIGO/Virgo posterior. In other words, while the retention of 3G BHs may be rare, any BHs that are retained will, by selection effects, have spins consistent

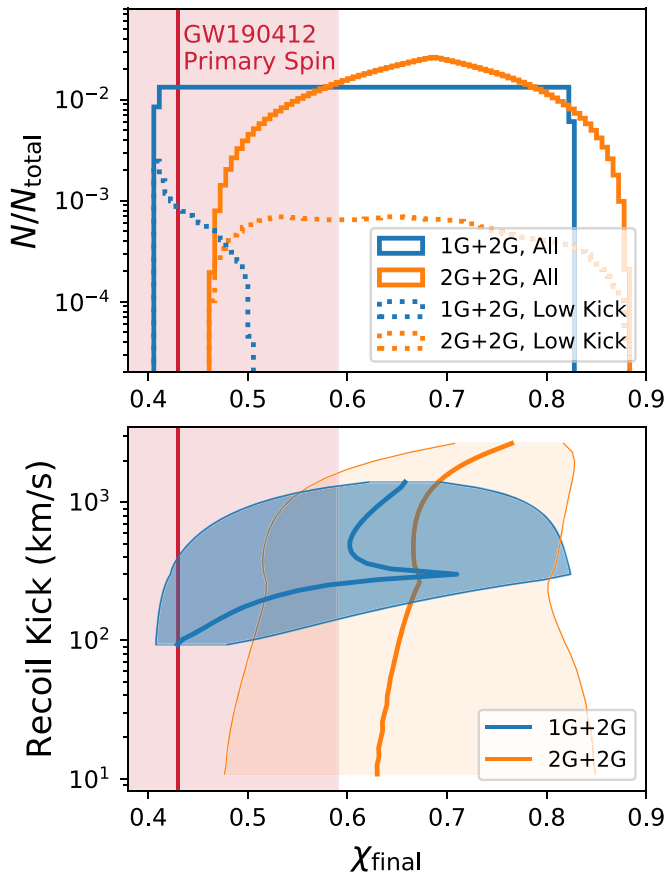


Figure 2. Creating GW190412 through the merger of 2G BHs. The top panel shows the distribution of spins for 3G BHs constructed according to the two schemes in Figure 1, with the full distribution shown with solid lines and the subset of systems that receive low recoil kicks ($\lesssim 100 \text{ km s}^{-1}$) shown with dashed lines. The bottom panel shows the relationship between the 3G BH spins and the recoil kicks they receive at birth, with the solid line and shaded regions showing the median and 90% regions of allowed final spins (assuming isotropic component spins at merger). The red line and shaded region indicate the median and 90% posterior on χ_1 for GW190412.

with the GW190412 primary. While the agreement between the final spins for 1G+2G mergers would suggest them as the primary source of GW190412-like binaries (especially since they are nearly 13 times more prevalent than 2G+2G mergers; Rodriguez et al. 2019), the minimum recoil speed produced by such binaries is nearly $\sim 90 \text{ km s}^{-1}$. This is greater than the escape speed from many nearby GCs and SSCs (although such clusters had significantly larger escape speeds in the past; see the top panel of Figure 3), suggesting that we must expand our search beyond typical Milky Way (MW) clusters.

3. Star Cluster Models

With a better understanding of the type of cluster most likely to form GW190412, we can search for similar events in high-fidelity models of dense star clusters. To that end, we use a series of star cluster models created with the Cluster Monte Carlo (CMC) code, a Hénon-style Monte Carlo code for stellar dynamics (Joshi et al. 2000, 2001; Fregeau et al. 2003; Fregeau & Rasio 2007; Umbreit et al. 2012; Chatterjee et al. 2010; Pattabiraman et al. 2013). In addition to the orbit-averaged Fokker–Planck diffusion of particles through phase space by two-body encounters (Hénon 1971, 1975), which drives the overall evolution of the cluster, CMC includes all of

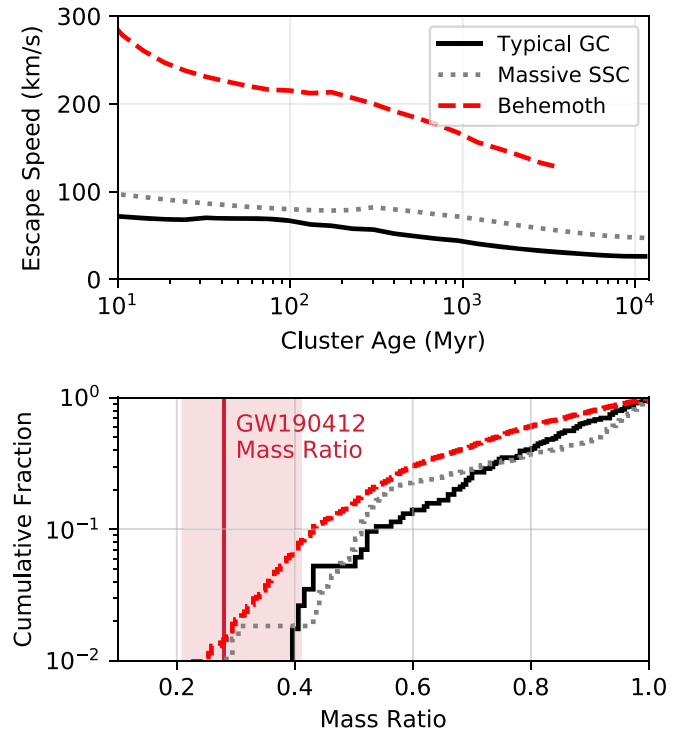


Figure 3. Top: the central escape speeds for a typical MW GC (with a metallicity of $Z = 0.002$ and a present-day mass of $\sim 2 \times 10^5 M_\odot$), a massive SSC that produces a GW190412-like binary ($Z = 0.02$ and final mass of $\sim 5 \times 10^5 M_\odot$ at the present day), both taken from Kremer et al. (2020), and behemoth, with metallicity $Z = 0.02$ and mass of $\sim 3 \times 10^6 M_\odot$ at its time of disruption, which produces several GW190412-like binaries. Bottom: the cumulative distribution of mass ratios for BBH mergers from the same three clusters, with the median and 90% mass ratio for GW190412 indicated in red.

the necessary physics for treating the formation, dynamics, ejections, and (multiple) mergers of BBH systems. This includes probabilistic formation of binaries through three-body BH encounters (Morscher et al. 2013), three- and four-body encounters performed by direct integration (Fregeau & Rasio 2007) and detailed stellar evolution prescriptions for stars and binaries using the binary stellar evolution (BSE) code of Hurley et al. (2000, 2002) with upgraded prescriptions for massive stellar winds and compact-object formation (Rodríguez et al. 2016c, 2018). In addition to the mergers of isolated BBHs arising from slow GW emission (either inside the cluster or after their ejection), CMC also follows the “prompt” merger of BBHs that are created by GW emission during two-body BH encounters in the cluster (following Samsing et al. 2019), and during three- and four-body strong encounters between binaries (Rodríguez et al. 2018). See Kremer et al. (2020) for a more detailed description. Note that we assume zero natal spins for 1G BHs (e.g., Fuller et al. 2019; Fuller & Ma 2019), and do not allow for spin up during BH–star mergers or mass transfer.

We use two sets of initial conditions for our analysis. The first is the CMC Cluster Catalog, a grid of models developed and presented in Kremer et al. (2020). Similar to previous studies, these models covered a wide range of initial particle numbers ($N = 2 \times 10^5, 4 \times 10^5, 8 \times 10^5, 1.6 \times 10^6$, and 3.2×10^6), cluster virial radii (0.5, 1, 2, and 4 pc), metallicities ($Z = 0.0002, 0.002$, and 0.02), and galactocentric distances (2, 8, and 20 kpc). Masses of stars are first taken from a Kroupa (2001) IMF, then 5% of stars are randomly assigned a binary companion with a mass drawn from a flat mass ratio

distribution between 0.1 and 1 and semimajor axes drawn from a uniform-in-log distribution (Duquennoy & Mayor 1991). Each model is integrated for 14 Gyr or until the cluster is dissolved.

We also consider one additional model, a massive SSC with a high metallicity named *behemoth*. Unlike previous CMC studies based on grids of parameters, this cluster is part of a new survey of realistic cluster initial conditions taken from FIRE-2 MHD cosmological simulations (Hopkins 2017; Hopkins et al. 2020); specifically, the cosmological formation of an L^* galaxy *m12i* (Wetzel et al. 2016). This new catalog will be presented fully in M. Grudic et al. (2020, in preparation). *Behemoth* has an initial 8.6×10^6 particles, 10% of which are binaries, for a total of 9.5×10^6 stars with stellar metallicities of $Z = 0.013$. Following the star formation and metallicity enrichment history of its host galaxy, *behemoth* is born at a redshift of 0.78, and unlike previous CMC models, experiences a time-dependent tidal potential based upon the orbit of a tracer particle within the *m12i* simulation.

To compute the tidal radius of the cluster, we follow a tracer particle associated with the cluster’s formation location within the *m12i* simulations. In each snapshot, we compute the local mass, velocity dispersion, and the tidal forces experienced by the particle. The effective tidal strength is calculated following Appendix D of Pfeffer et al. (2018). This value is then implemented as the tidal truncation in CMC, where we strip any star whose apocenter moves beyond this boundary.

The tracer particle of *behemoth* does not experience dynamical friction, so we must add it in postprocessing. To that end, we again follow Pfeffer et al. (2018) and compute the instantaneous timescale for dynamical friction to bring the cluster into its galactic center (Lacey & Cole 1993) as

$$T_{\text{df}} = \frac{\epsilon^{0.78}}{2B(v_c/\sqrt{2}\sigma)} \frac{\sqrt{2}\sigma r^2}{GM_c \log\Lambda}, \quad (1)$$

where r is the radius of the orbit in the galaxy, M_c is the cluster mass as a function of time, v_c is the circular velocity of a particle at radius r , $B(x) = \text{erf}(x) - 2x \exp(-x^2)/\sqrt{\pi}$ is the standard dynamical friction velocity expression (e.g., Binney & Tremaine 2008). ϵ is the eccentricity correction from Lacey & Cole (1993), defined as the ratio of the angular momentum of the particle to that of a particle on a circular orbit with the same energy. Finally, $\log\Lambda$ is the Coulomb logarithm, where $\Lambda = 1 + M_c/M_{\text{enc}}$, and M_{enc} is mass of the galaxy interior to r . We integrate *behemoth* until the cumulative number of dynamical friction times is greater than the age of the cluster, i.e.,

$$\int \frac{dt}{T_{\text{df}}} > 1. \quad (2)$$

Once (2) is satisfied, we assume the cluster has spiraled into its galactic center. For *behemoth*, this happens at redshift 0.22, approximately 4.2 Gyr after the cluster’s formation.

Behemoth is the largest cluster model created with CMC, and exhibits some unique properties. A typical GC produces ~ 100 BBHs over a ~ 12 – 13 Gyr lifetime, approximately half of which will be ejected from the cluster prior to merger (e.g., Rodríguez et al. 2016c, 2018). But *behemoth* creates 1300 BBH mergers over its 4.2 Gyr lifetime, 90% of which merge inside the cluster. This increase in the fraction of in-cluster mergers is largely due to the large central escape speed of the

cluster, initially in excess of 300 km s^{-1} . As a result, 36% of BBH mergers from *behemoth* have at least one component created in a previous merger. This increase in both in-cluster mergers and higher generation BHs has been noted before in semianalytic models of massive clusters such as NSCs (e.g., Miller & Lauburg 2009; Antonini & Rasio 2016), but this is the first time it has been demonstrated in fully collisional cluster simulations.

4. Forming GW190412-like Binaries

We begin by searching both the grid of models and *behemoth* for merging binaries whose m_1 and m_2 lie within the 90% credible regions for GW190412. From the CMC grid, we identify 39 such systems that merge within a Hubble time, 36 of which originate from high-metallicity ($Z = 0.02$) clusters. 34 of these systems are produced through repeated BH mergers, and as such have spinning primaries. However, no individual cluster matches *behemoth*: the massive cluster produces 14 BBH mergers with masses similar to GW190412 over its 4.2 Gyr lifetime, all of which are the result of multiple BH mergers. The majority of these systems are 1G+2G mergers with mass ratios that sit near the upper 90% region of the GW190412 mass ratio posterior and primary spins of ~ 0.69 . *Behemoth* produces three to four times more low-mass-ratio events than a typical GC or massive SSC (Figure 3, bottom panel) with 8% of BBHs having mass ratios consistent with GW190412.

There are many clusters that can produce BBHs with component masses similar to GW190412. However, imposing the requirement that the spin magnitude of the primary matches the LIGO/Virgo posterior tells a different story. Limiting our sample to only those binaries where the primary BH has spin magnitude between 0.17 and 0.59, we find only four potential GW190412 progenitors, all of which are 3G+1G BBHs. Of these, three were created in *behemoth* through the 1G+2G channel described in Section 2, which required an escape speed $\gtrsim 90 \text{ km s}^{-1}$. Only one system, where a chance 2G+2G merger experienced a low-recoil kick and was retained by its parent cluster, was produced in the entire cluster grid from Kremer et al. (2020), despite the grid having more than 10 times the total stellar mass of *behemoth*. As expected, this merger occurred in a massive, high-metallicity cluster with $Z = 0.02$ and an initial mass of $\sim 10^6 M_\odot$. However, the central escape speed of this cluster (shown in Figure 3) falls below the 90 km s^{-1} threshold for the 1G+2G pathway within tens of megayears of its birth, before the first dynamically assembled BBHs begin to merge. It is only in the most massive of high-metallicity clusters where the 1G+2G process for creating GW190412-like binaries can occur. We show merger trees for the four BBH systems, including their masses, spins, recoil speeds, and Local Cluster escape speeds, in Figure 4.

It is nearly impossible to estimate the volumetric rate of 3G+1G mergers like GW190412 using a handful of mergers from two cluster models, and even back-of-the-envelope estimates provide limited clarity. However, we can proceed as follows: for the CMC Cluster Catalog, we compute a cosmological merger time for each BBH by adding its CMC-computed merger time to a randomly drawn cluster birth redshift based on the metallicity of its host, using the semianalytic GC formation models of El-Badry et al. (2019). These BBH merger times are then combined with the BBHs from *behemoth*, whose merger times are determined by the combination of internal dynamics

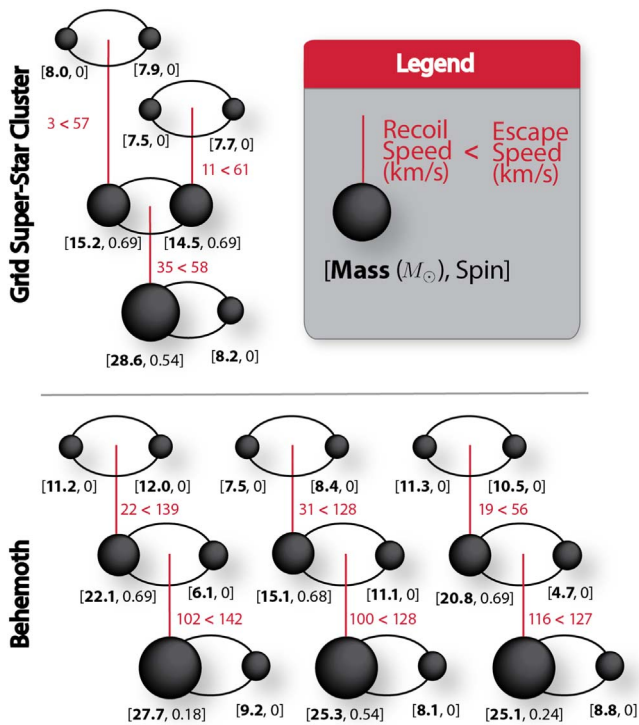


Figure 4. BH merger trees that form GW190412-like binaries. The pairs of numbers under each BH show the mass (in M_{\odot}) and spin, while the inequalities show the GW recoil of each merging binary as being less than the Local Cluster escape speed (in km s^{-1}) where the merger occurs. The top tree shows the one BBH formed through a 2G+2G merger in the grid of cluster models described in Kremer et al. (2020), while the bottom three trees show the mergers that occur in *behemoth*, where the large escape speed allows for the retention of 1G+2G merger products.

and the cluster’s birth redshift in the *m12i* simulation.⁸ This population yields 1757 total BBH mergers at $z \lesssim 0.5$, of which 54 have mass ratios $\lesssim 0.41$ (39 of which are produced by *behemoth*). If we restrict ourselves to binaries whose masses individually match the GW190412 posterior probability distribution, we are left with five BBHs from *behemoth* and three from the CMC Cluster Catalog. Restricting ourselves further to those whose masses and spins match the GW posterior, only the three BBH systems from *behemoth*, illustrated in Figure 4, remain. If we assume a merger rate of $\lesssim 20 \text{ Gpc}^{-3} \text{ yr}^{-1}$ from clusters at $z < 0.5$ (Rodríguez & Loeb 2018, Figure 1), this suggests relative merger rates of $\sim 0.6 \text{ Gpc}^{-3} \text{ yr}^{-1}$ for BBHs with mass ratios less than 0.41, $\sim 0.09 \text{ Gpc}^{-3} \text{ yr}^{-1}$ for BBHs with GW190412-like m_1 and m_2 , and $\sim 0.03 \text{ Gpc}^{-3} \text{ yr}^{-1}$ for BBHs with m_1 , m_2 , and χ_1 all consistent with GW190412.

However, the initial conditions for the CMC Cluster Grid are based upon star clusters in the MW. *Behemoth* is decidedly not a typical present-day MW star cluster, globular or otherwise. Its central escape speed is more than 200 km s^{-1} after 130 Myr, when it begins to dynamically produce BBH mergers, and remains above 150 km s^{-1} after 2 Gyr, when the production of GW190412-like binaries begins. There are no clusters with central escape speeds in the MW, where even the largest GCs have central escape speeds $\lesssim 125 \text{ km s}^{-1}$ (Gnedin et al. 2002). However, SSCs with comparable masses and

escape velocities are observed in nearby galaxies. In NGC 3034, the cluster SSC-L has a virial mass of $4 \times 10^6 M_{\odot}$ (McCradly & Graham 2007) and an effective radius of 1.45 pc (assuming a distance of 3.6 Mpc, McCradly et al. 2003), suggesting a central escape speed of 154 km s^{-1} .⁹ NGC 34 and NGC 1316 contain clusters S1 (Schweizer & Seitzer 2007) and G114 (Bastian et al. 2006) respectively, which have masses of $\sim 2 \times 10^7 M_{\odot}$, and effective radii $\lesssim 5 \text{ pc}$,¹⁰ suggesting $v_{\text{esc}}^{\text{center}} \gtrsim 180 \text{ km s}^{-1}$ for both clusters. Finally, the cluster W3 in NGC 7252 has a mass of nearly $\sim 10^8 M_{\odot}$ and an effective radius of 17.5 pc, with Cabrera-Ziri et al. (2016) calculating a central escape speed anywhere from 193 to 254 km s^{-1} .

Each of the aforementioned clusters have sufficiently large $v_{\text{esc}}^{\text{center}}$ to enable the formation of GW190412-like binaries through the channels illustrated in Figure 4. Furthermore, although no such *behemoth*-like clusters exist in the MW, this may be because any such clusters would have spiraled into the Galactic center many gigayears ago (e.g., Gnedin & Ostriker 1997). The cluster’s birth properties and survival time are strongly dependent on the properties of its host galaxy, such as its star formation rate, tidal field, and metallicity enhancement. Unlike previous rate estimates of BBH mergers from star clusters (e.g., Portegies Zwart & Mcmillan 2000; Askar et al. 2016; Rodríguez et al. 2016c; Choksi et al. 2018; Hong et al. 2018), this Letter suggests that the production rate of GW190412-like binaries likely depends on clusters that may no longer exist in the MW and many other galaxies. Only a handful of analytic studies (e.g., Fragione & Kocsis 2018) have considered the contribution of such massive clusters that no longer exist, and they find that the contribution from such systems is similar to the contribution from all other clusters combined.

5. Conclusion

In this Letter, we argued that if the recent LIGO/Virgo BBH, GW190412, were formed through classical three-body encounters in a dense star cluster, then it was likely the product of two successive BH merger events. Using a combination of analytic prescriptions for BBH recoils and spins, and a series of collisional models of dense star clusters (including a new, massive cluster, *behemoth*), we show that the primary of GW190412 is typical of BHs formed from the merger of two $\sim 10 M_{\odot}$ BHs, whose merger product then merges with another $\sim 10 M_{\odot}$ BH. While such events are rare, we show that any such mergers retained by the cluster would naturally have masses and spins similar to the components of GW190412. Although this requires a cluster with an escape speed of at least 90 km s^{-1} , such clusters are known to exist in nearby galaxies, and may have existed in the MW before being destroyed by dynamical friction.

Although we have focused on dynamical formation in unusually large clusters, such as SSCs, there is every reason to expect that similar processes operate in potentially higher numbers in the NSCs that reside in the centers of galaxies. For systems without central massive BHs, the higher central escape

⁹ Here we calculate the central escape speed as $v_{\text{esc}}^{\text{center}} = \sqrt{2GM_c/r_{\text{eff}}}$, where M_c is the cluster mass and r_{eff} is the effective radius, or the projected half-mass-radius. For a Plummer sphere, this relation is exact; see Heggie & Hut (2003, p. 81).

¹⁰ For S1, the effective radius is inferred to be less than 5 pc based on comparisons to clusters in NGC 3921 (Schweizer et al. 2004), while Bastian et al. (2006) report a best-fit r_{eff} for G114 of 4.08 pc.

⁸ Though we note that the formation redshift of *behemoth* in the *m12i* simulation, $z = 0.78$, is very similar to what El-Badry et al. (2019) would predict for a similarly high-metallicity cluster ($z = 0.81$).

speeds of NSCs can facilitate many generations of BH mergers (e.g., Antonini & Rasio 2016), beyond even the three considered here. Multiple BH mergers are also easily achievable in environments around supermassive BHs, where the high velocity and escape speeds ($\gtrsim 10^3 \text{ km s}^{-1}$) can retain many generations of BHs, whether their progenitor binaries formed through GW-assisted captures (O’Leary et al. 2009) in BH cusps or through gas-assisted captures in AGN disks (e.g., Yang et al. 2019a, 2019b). We note that the initial escape speed of behemoth, 300 km s^{-1} , approaches the speed required for a collisional runaway of BHs that may form an intermediate-mass BH (Antonini et al. 2019). However, clusters with central BHs have distinct dynamical features, including high central velocity dispersions, which may actually inhibit the formation of stellar-mass BBHs through three-body encounters (the rate of which scales as $1/\sigma^9$; Ivanova et al. 2005). Unfortunately, star-by-star models of NSC dynamics are still beyond the capabilities of the current generation of direct N -body and Henón Monte Carlo codes, making such models difficult to study in detail. Despite this, significant progress has been made in semianalytic treatments of the hierarchical BBH merger problem (e.g., Gerosa & Berti 2019; Arca Sedda et al. 2020; Doctor et al. 2020; Kimball et al. 2020a, 2020b).












Throughout this paper, we have assumed that all BHs born from stellar collapse are born with zero spins. However, if 1G BHs were born spinning, then it is entirely possible that the only 2G BHs that would be retained are those with spins similar to GW190412. As this manuscript was being completed, we learned of a similar study by Gerosa et al. (2020) exploring this scenario. There, the authors use similar semianalytic arguments and GW parameter-estimation techniques to study a hierarchical merger scenario for GW190412. Although they focus on 1G+2G mergers (with varying spins for 1G BHs) as opposed to our 1G+3G scenario, they similarly conclude that producing a GW190412-like BBH through a hierarchical merger scenario would require a cluster with an escape speed $\gtrsim 150 \text{ km s}^{-1}$. It is also possible that, if 1G BHs are born with substantial spins, then GW190412 could have originated from a chance low-mass-ratio 1G+1G merger. We identified five such mergers in the CMC Cluster Catalog, suggesting the rate of such events, if 1G BHs were born spinning, is $\sim 0.06 \text{ Gpc}^{-3} \text{ yr}^{-1}$.

The mass of behemoth approaches that of some central star clusters in dwarf galaxies, suggesting that many interesting BBH mergers may arise from the dividing line between massive GCs, SSCs, and NSCs in galactic centers. In this case, the tidal forces and galactic environment did not play a significant role in the cluster evolution; the mass, metallicity, and dynamical-friction timescale were the main features contributing to the production of BBH outliers like GW190412. However, for many clusters, the complicated relationship between clusters and their host galaxies, including a careful treatment of dynamical friction and tidal forces, must be correctly addressed (see e.g., Choksi & Kruijssen 2019). Efforts to perform zoom-in collisional cluster simulations from cosmological initial conditions are currently underway (M. Grudic et al. 2020, in preparation; C. Rodríguez et al. 2020, in preparation).

C.R. thanks Hanfei Cui and Peter Phan, participants in the Science Research Mentoring Program (SRMP) at the Center for Astrophysics Harvard & Smithsonian, as well as the

anonymous referee, for useful discussions. C.R. was supported by an ITC Postdoctoral Fellowship from Harvard University. M.G. and G.F. acknowledge support from a CIERA Fellowship at Northwestern University. This work was supported in part by NSF Grant AST-1716762 at Northwestern University. S.C. acknowledges support of the Department of Atomic Energy, Government of India, under project no. 12-R&D-TFR-5.02-0200. A.L. acknowledges funding from the Observatoire de la Côte d’Azur and the Centre National de la Recherche Scientifique through the Programme National des Hautes Energies and the Programme National de Physique Stellaire. The computations in this paper were run on the FASRC Cannon cluster supported by the FAS Division of Science Research Computing Group and by the black hole Initiative (funded by JTF and GBMF grants), both at Harvard University, and on the San Diego Supercomputing Center Comet cluster under allocation PHY180017 granted by the Extreme Science and Engineering Discovery Environment (XSEDE), supported by the NSF (ACI-1548562).

ORCID iDs

Carl L. Rodríguez  <https://orcid.org/0000-0003-4175-8881>
 Kyle Kremer  <https://orcid.org/0000-0002-4086-3180>
 Michael Y. Grudic  <https://orcid.org/0000-0002-1655-5604>
 Zachary Hafen  <https://orcid.org/0000-0001-7326-1736>
 Sourav Chatterjee  <https://orcid.org/0000-0002-3680-2684>
 Giacomo Fragione  <https://orcid.org/0000-0002-7330-027X>
 Astrid Lamberts  <https://orcid.org/0000-0001-8740-0127>
 Miguel A. S. Martinez  <https://orcid.org/0000-0001-5285-4735>
 Frederic A. Rasio  <https://orcid.org/0000-0002-7132-418X>
 Newlin Weatherford  <https://orcid.org/0000-0002-9660-9085>
 Claire S. Ye  <https://orcid.org/0000-0001-9582-881X>

References

- Aasi, J., Abbott, B. P., Abbott, R., et al. 2015, *CQGra*, **32**, 074001
 Abbott, B. P., Abbott, R., Abbott, T. D., et al. 2016, *ApJL*, **818**, L22
 Abbott, B. P., Abbott, R., Abbott, T. D., et al. 2019a, *ApJL*, **882**, L24
 Abbott, B. P., Abbott, R., Abbott, T. D., et al. 2019b, *PhRvX*, **9**, 031040
 Acernese, F., Agathos, M., Agatsuma, K., et al. 2015, *CQGra*, **32**, 024001
 Antonini, F., Gieles, M., & Gualandris, A. 2019, *MNRAS*, **486**, 5008
 Antonini, F., & Rasio, F. A. 2016, *ApJ*, **831**, 187
 Arca Sedda, M., Mapelli, M., Spera, M., Benacquista, M., & Giacobbo, N. 2020, arXiv:2003.07409
 Askar, A., Szkudlarek, M., Gondke-Rosińska, D., Giersz, M., & Bulik, T. 2016, *MNRAS*, **464**, L36
 Barausse, E., & Rezzolla, L. 2009, *ApJL*, **704**, L40
 Bartos, I., Kocsis, B., Haiman, Z., & Márka, S. 2017, *ApJ*, **835**, 165
 Bastian, N., Saglia, R. P., Goudfrooij, P., et al. 2006, *A&A*, **448**, 881
 Belczynski, K., Dominik, M., Bulik, T., et al. 2010, *ApJL*, **715**, L138
 Belczynski, K., Klencki, J., Fields, C. E., et al. 2020, *A&A*, **636**, A104
 Berti, E., Cardoso, V., Gonzalez, J. A., et al. 2007, *PhRvD*, **76**, 064034
 Berti, E., & Volonteri, M. 2008, *ApJ*, **684**, 822
 Binney, J., & Tremaine, S. 2008, *Galactic Dynamics* (Princeton, NJ: Princeton Univ. Press) publication Title: (Second Edition)
 Cabrera-Ziri, I., Bastian, N., Hilker, M., et al. 2016, *MNRAS*, **457**, 809
 Campanelli, M., Lousto, C., Zlochower, Y., & Merritt, D. 2007, *ApJL*, **659**, L5
 Chatterjee, S., Fregeau, J. M., Umbreit, S., & Rasio, F. A. 2010, *ApJ*, **719**, 915
 Chatterjee, S., Rodríguez, C. L., Kalogera, V., & Rasio, F. A. 2017, *ApJL*, **836**, L26
 Choksi, N., Gnedin, O. Y., & Li, H. 2018, *MNRAS*, **480**, 2343
 Choksi, N., & Kruijssen, J. M. D. 2019, arXiv:1912.05560
 De Mink, S. E., & Mandel, I. 2016, *MNRAS*, **460**, 3545
 Di Carlo, U. N., Mapelli, M., Giacobbo, N., et al. 2020, arXiv:2004.09525
 Doctor, Z., Wysocki, D., O’Shaughnessy, R., Holz, D. E., & Farr, B. 2020, *ApJ*, **893**, 35

- Dominik, M., Belczynski, K., Fryer, C., et al. 2012, *ApJ*, 759, 52
- Duquennoy, A., & Mayor, M. 1991, *A&A*, 500, 337
- El-Badry, K., Quataert, E., Weisz, D. R., Choksi, N., & Boylan-Kolchin, M. 2019, *MNRAS*, 482, 4528
- Fishbach, M., Holz, D. E., & Farr, B. 2017, *ApJL*, 840, L24
- Fragione, G., & Kocsis, B. 2018, *PhRvL*, 121, 161103
- Fregeau, J. M., Gürkan, M. A., Joshi, K. J., & Rasio, F. A. 2003, *ApJ*, 593, 772
- Fregeau, J. M., & Rasio, F. A. 2007, *ApJ*, 658, 1047
- Fuller, J., & Ma, L. 2019, *ApJL*, 881, L1
- Fuller, J., Piro, A. L., & Jermyn, A. S. 2019, *MNRAS*, 485, 3661
- Gerosa, D., & Berti, E. 2017, *PhRvD*, 95, 124046
- Gerosa, D., & Berti, E. 2019, *PhRvD*, 100, 041301
- Gerosa, D., Vitale, S., & Berti, E. 2020, arXiv:2005.04243
- Gnedin, O. Y., & Ostriker, J. P. 1997, *ApJ*, 474, 223
- Gnedin, O. Y., Zhao, H., Pringle, J. E., et al. 2002, *ApJL*, 568, L23
- González, J. A., Spherhake, U., Brüggemann, B., Hannam, M., & Husa, S. 2007, *PhRvL*, 98, 091101
- Harris, W. E. 1996, *AJ*, 112, 1487
- Hénon, M. 1971, *Ap&SS*, 14, 151
- Hénon, M. 1975, in IAU Symp. 69, Dynamics of the Solar Systems, ed. A Hayli (Dordrecht: Reidel), 133
- Hong, J., Vesperini, E., Askar, A., et al. 2018, *MNRAS*, 480, 5645
- Hopkins, P. F. 2017, arXiv:1712.01294
- Hopkins, P. F., Chan, T. K., Garrison-Kimmel, S., et al. 2020, *MNRAS*, 492, 3465
- Hurley, J. R., Pols, O. R., & Tout, C. A. 2000, *MNRAS*, 315, 543
- Hurley, J. R., Tout, C. A., & Pols, O. R. 2002, *MNRAS*, 329, 897
- Heggie, D., & Hut, P. (ed.) 2003, The Gravitational Million-Body Problem: A Multidisciplinary Approach to Star Cluster Dynamics (Cambridge: Cambridge Univ. Press), 372
- Hut, P., & Bahcall, J. N. 1983, *ApJ*, 268, 319
- Ivanova, N., Belczynski, K., Fregeau, J. M., & Rasio, F. A. 2005, *MNRAS*, 358, 572
- Joshi, K. J., Nave, C. P., & Rasio, F. A. 2001, *ApJ*, 550, 691
- Joshi, K. J., Rasio, F. A., Zwart, S. P., & Portegies Zwart, S. 2000, *ApJ*, 540, 969
- Kesden, M., Spherhake, U., & Berti, E. 2010, *PhRvD*, 81, 084054
- Kimball, C., Berry, C., & Kalogera, V. 2020a, *RNAAS*, 4, 2
- Kimball, C., Talbot, C., Berry, C. P. L., et al. 2020b, arXiv:2005.00023
- Kremer, K., Ye, C. S., Rui, N. Z., et al. 2020, *ApJS*, 247, 48
- Kroupa, P. 2001, *MNRAS*, 322, 231
- Kulkarni, S. R., Hut, P., & McMillan, S. J. 1993, *Natur*, 364, 421
- Lacey, C., & Cole, S. 1993, *MNRAS*, 262, 627
- Lousto, C. O., & Zlochower, Y. 2008, *PhRvD*, 77, 044028
- Lousto, C. O., & Zlochower, Y. 2013, *PhRvD*, 87, 084027
- Lousto, C. O., Zlochower, Y., Dotti, M., & Volonteri, M. 2012, *PhRvD*, 85, 084015
- Mandel, I., & Fragos, T. 2020, *ApJL*, 895, L28
- McCraday, N., Gilbert, A. M., & Graham, J. R. 2003, *ApJ*, 596, 240
- McCraday, N., & Graham, J. R. 2007, *ApJ*, 663, 844
- McKernan, B., Ford, K. E. S., O'Shaughnessy, R., & Wysocki, D. 2020, *MNRAS*, 494, 1203
- Miller, M. C., & Lauburg, V. M. 2009, *ApJ*, 692, 917
- Morscher, M., Pattabiraman, B., Rodríguez, C., Rasio, F. A., & Umbreit, S. 2015, *ApJ*, 800, 9
- Morscher, M., Umbreit, S., Farr, W. M., & Rasio, F. A. 2013, *ApJL*, 763, L15
- Nitz, A. H., Dent, T., Davies, G. S., et al. 2020, *ApJ*, 891, 123
- O'Leary, R. M., Kocsis, B., & Loeb, A. 2009, *MNRAS*, 395, 2127
- Olejak, A., Belczynski, K., Holz, D. E., et al. 2020, arXiv:2004.11866
- Pattabiraman, B., Umbreit, S., Liao, W.-K., et al. 2013, *ApJSS*, 204, 15
- Pfeffer, J., Kruijssen, J. M. D., Crain, R. A., & Bastian, N. 2018, *MNRAS*, 475, 4309
- Portegies Zwart, S. F., McMillan, S. L., & Gieles, M. 2010, *ARA&A*, 48, 431
- Portegies Zwart, S. F., & Mcmillan, S. L. W. 2000, *ApJ*, 528, 17
- Rodríguez, C. L., Amaro-Seoane, P., Chatterjee, S., & Rasio, F. A. 2018, *PhRvL*, 120, 151101
- Rodríguez, C. L., Chatterjee, S., & Rasio, F. A. 2016a, *PhRvD*, 93, 084029
- Rodríguez, C. L., Haster, C.-J., Chatterjee, S., Kalogera, V., & Rasio, F. A. 2016b, *ApJL*, 824, L8
- Rodríguez, C. L., & Loeb, A. 2018, *ApJL*, 866, L5
- Rodríguez, C. L., Morscher, M., Wang, L., et al. 2016c, *MNRAS*, 463, 2109
- Rodríguez, C. L., Zevin, M., Amaro-Seoane, P., et al. 2019, *PhRvD*, 100, 043027
- Samsing, J., D'Orazio, D. J., Kremer, K., Rodríguez, C. L., & Askar, A. 2019, arXiv:1907.11231
- Schweizer, F., & Seitzer, P. 2007, *AJ*, 133, 2132
- Schweizer, F., Seitzer, P., & Brodie, J. P. 2004, *AJ*, 128, 202
- Secunda, A., Bellovary, J., Mac Low, M.-M., et al. 2019, *ApJ*, 878, 85
- Sigurdsson, S., & Hernquist, L. 1993, *Natur*, 364, 423
- Sigurdsson, S., & Phinney, E. S. 1993, *ApJ*, 415, 631
- Spera, M., Mapelli, M., & Bressan, A. 2015, *MNRAS*, 451, 4086
- Stone, N. C., Metzger, B. D., & Haiman, Z. 2017, *MNRAS*, 464, 946
- The LIGO Scientific Collaboration, & the Virgo Collaboration 2020, arXiv:2004.08342
- Tichy, W., & Marronetti, P. 2008, *PhRvD*, 78, 081501
- Umbreit, S., Fregeau, J. M., Chatterjee, S., & Rasio, F. A. 2012, *ApJ*, 750, 31
- Venumadhav, T., Zackay, B., Roulet, J., Dai, L., & Zaldarriaga, M. 2020, *PhRvD*, 101, 083030
- Vink, J. S., de Koter, A., & Lamers, H. J. G. L. M. 2001, *A&A*, 369, 574
- Wetzel, A. R., Hopkins, P. F., Kim, J.-H., et al. 2016, *ApJL*, 827, L23
- Yang, Y., Bartos, I., Gayathri, V., et al. 2019a, *PhRvL*, 123, 181101
- Yang, Y., Bartos, I., Haiman, Z., et al. 2019b, *ApJ*, 876, 122
- Ye, C. S., Fong, W.-f., Kremer, K., et al. 2020, *ApJL*, 888, L10